Helium-ion-induced fission excitation functions of terbium and ytterbium

R. H. Iyer, A. K. Pandey, P. C. Kalsi, and R. C. Sharma
Radiochemistry Division, Bhabha Atomic Research Centre, Trombay, Bombay–400 085, India
(Received 15 December 1992)

^{4}He-ion-induced fission excitation functions of terbium ($Z=65$) and ytterbium ($Z=70$) were obtained by measuring fission cross sections in the energy range of 40–65 MeV using lexan polycarbonate plastic as the fission fragment track detector. The present measurements extend the range of low-Z elements in the deformed region for which ^{4}He-ion-induced fission excitation functions were obtained at moderate energies. The analysis of the ratio of $\Gamma_f/\Gamma_n \approx \sigma_f/\sigma_R$, which is a measure of the competition between fission and neutron emission widths, in terms of the statistical model expression, indicates the fission thresholds for ^{163}Ho and $^{177.1}$Hf to be 31.5±3.5 and 26.7±3.0 MeV, respectively. The corresponding value for the fission level density parameter a_f was found to be $A/12$ MeV^{-1} for both the compound nuclei. $^{163}_{67}$Ho represents the lightest compound nucleus for which fission barrier has been determined experimentally. The measured fission barriers compare very well with the theoretical fission barriers obtained by liquid-drop-based models. The present data have been used along with similar data available in the literature to bring out some systematics in the fission properties of low-Z elements. A systematic trend was observed in the a_f/a_n ratio of preactinide elements ranging from ^{163}Ho to ^{213}At (16 nuclei). A linear dependence of $\log_{10}\Gamma_f/\Gamma_n$ with Z^2/A at constant excitation energies was observed extending over 8 orders of magnitude for low Z-compound nuclear systems from ^{163}Ho to ^{213}At all of which are characterized by a predominance of symmetric fission. A linear dependence was also observed in the variation of $\log_{10}\Gamma_f/\Gamma_n$ with $E_f'-B_n'$ where E_f' is the effective fission barrier and B_n', neutron binding energy including 50% shell correction and pairing energy term, at constant excitation energies (40 MeV) for these 16 low-Z compound nuclear systems. The results suggest that shell effects tend to persist even at excitation energies of 40 MeV. An analysis was also done to separate the symmetric and asymmetric fission barriers. It is observed that asymmetric fission barrier E_f(asym) is much higher than symmetric fission barrier E_f(sym) for $A \leq 200$ clearly suggesting that symmetric fission is the only observable mode below compound nuclear mass $A=200$.

PACS number(s): 25.55.−e, 25.85.Ge

INTRODUCTION

One of the main objectives of the present work is to study the effects of ground-state deformation on fission properties and also to understand some aspects of the systematics of the fission of lighter elements ($Z \leq 80$). This work is an extension of our earlier work [1] and extends the range of low-Z elements that are away from the closed-shell region and whose fission properties are studied experimentally at moderate excitation energies. The importance of studies of fission properties of low-Z elements in the present work is that these elements have large ellipticity (Q/ZR^2; where Q = quadrupole moment, Z = nuclear charge, and R = radius) or permanent ground-state distortion [2]. Hill and Wheeler [3] predicted that the same factors which cause large quadrupole moments could be expected to lower the fission barrier height by a few MeV. Although the same effect should be present in the fission of distorted heavy elements ($Z \geq 90$), the effect of ground-state distortion may not be observable because greater than 80% of the total cross section already leads to fission, even at modest excitation energies. Since the expected fission cross sections of lighter elements ($Z \leq 80$) are extremely low (i.e., nanobarns), it would appear that even small effects of ground-state distortion on the fission barrier might be seen around $Z \approx 70$ from studies of neighboring nuclides where elements have large ground-state deformation. Moreover, reliable and accurate measurements of fission barriers (particularly in the lighter elements below lead) which are equivalent to measurement of nuclear masses at a distorted "saddle-point configuration" not only help in the understanding of the systematics of fission process but also would enhance our understanding of the systematics of nuclear masses in general [4]. The fission studies on a range of low-Z elements induced by intermediate-energy (< 100 MeV) charged particles also provide excellent opportunities for determining important nuclear parameters, such as fission barriers (E_f), level-density parameters for neutron emission (a_n) and fission (a_f), influence of shell effects, etc., by analyzing the fission excitation functions, and for comparing these parameters with predictions of theoretical models [5]. Using a glass detector, Kuvatov *et al.* [6] reported results of fission cross sections and fragment angular anisotropies in the 38-MeV He-ion-induced fission of several nuclei in the region $Z=73-83$ and have made some interesting observations on the systematics of a_f and a_n in the low-Z element region. In the variation of a_f/a_n as a function of Z^2/A, they found a structure with a maximum in the region of nuclei near the closed shell and a minimum in the nuclei near the deformed region. The structure is absent

in fissioning systems induced by heavy ions [7], with large excitation energies of 50–100 MeV, where the role of shells is already small. The role of shell effects on the level-density parameter (a_f/a_n ratio) can be understood more clearly by extending the measurements in the range of nuclei away from the closed-shell configuration. The present work is also aimed at more clearly defining the observed linear dependence of $\log_{10}\Gamma_f/\Gamma_n$ with Z^2/A in our earlier reported work [1] in the lighter-element region, e.g., ^{169}Tm; more so because of statistical uncertainties associated with measurements of such low fission cross sections.

In this paper, we report the results of our work on the fission excitation functions of natural ytterbium ($Z=70$) and terbium ($Z=65$) induced by He ions in the energy range of 40–65 MeV from the Variable Energy Cyclotron at Calcutta and using identical techniques and procedures reported in our earlier publication [1]. The present data along with similar data available in the literature have been used to bring out some interesting predictions concerning the trends and systematics of symmetric and asymmetric fission barriers in the lighter and heavier nuclei. Some preliminary results of this work have been reported previously [8].

EXPERIMENTAL PROCEDURES

Details of the procedures for purification and preparation of the targets and backing foils, irradiation, data evaluation, etc., are given elsewhere [1] and are given here briefly. The thin uniform targets were prepared from high-purity Tb_2O_3 and Yb_2O_3 (obtained from M/s, Johnson Mathey Chemicals Ltd., England and repurified by us through an ion-exchange separation scheme) on high-purity silver foils in the form of deposits of 1–2 mg/cm^2 thickness. The maximum heavy-element contamination was estimated to be no more than 3–5 parts per billion (ppb) in the final prepared targets. The fission fragments recoiling in the backward direction were recorded using a cylindrical lexan detector. Total integrated beam currents of the order of 1–2 μA h were used in each experiment. Lutetium and gold targets were used as reference standards as their absolute fission cross sections as a function of He-ion energy are known [1].

EXPERIMENTAL RESULTS

The measured total fission cross sections, for the helium-ion-induced fission of $^{159}_{69}$Tb and natural $^{173.1}_{70}$Yb (0.135% ^{168}Yb, 3.03% ^{170}Yb, 14.31% ^{171}Yb, 21.82% ^{172}Yb, 16.13% ^{173}Yb, 31.84% ^{174}Yb, and 12.73% ^{176}Yb) are given in Table I. The excitation energies were calculated by assuming full momentum transfer and using a Q value of -0.7 MeV for the ^{159}Tb+^{4}He reaction and -2.2 MeV for the $^{173.1}$Yb+^{4}He reaction, which are calculated from the mass tables of Myers and Swiatecki [9]. Only the statistical errors involved in track counting for measurements of fission cross section are given in Table I. The other sources of errors include those arising from variations in target thickness, heavy-element contamination, integrated beam current, focusing of the beam on the centers of the targets, which may cause errors in solid-angle calculation, and variation of track densities along the length of the detector film (see Fig. 1 of Ref. [1]), uncertainties in the reference fission cross section, etc. The overall accuracy of the results of the $^{173.1}$Yb+^{4}He reaction is estimated to be about 20%. For the ^{159}Tb+^{4}He reaction, the accuracy of the results is estimated to be 20% at all the ion energies above 50 MeV and about 50% at lower energies.

DISCUSSION

The data were analyzed using the statistical model expression suggested by Vandenbosch and Huizenga [5], which is the most appropriate method of analyzing fission excitation functions of low-Z elements.

$$\frac{\Gamma_f}{\Gamma_n}=\frac{K_0 a_n[2a_f^{1/2}(E-E_f)^{1/2}-1]}{4a_f A^{2/3}(E-B_n)} \times\exp[2a_f^{1/2}(E-E_f)^{1/2}-2a_n^{1/2}(E-B_n)^{1/2}]$$

where a_n and a_f are level density parameters for neutron emission and fission, respectively, E is the excitation ener-

TABLE I. Experimental fission cross sections for terbium and ytterbium.

Target	^{4}He ion energy (MeV)	Excitation energy (MeV)	Measured fission cross section, σ_f (cm^2)	Calculated reaction cross section, σ_R (cm^2)	$\Gamma_f/\Gamma_n \approx \sigma_f/\sigma_R$
^{159}Tb	47.5	45.6	$(4.16\pm0.91)\times10^{-33}$	1.910×10^{-24}	2.178×10^{-9}
	50.0	48.0	$(1.54\pm0.28)\times10^{-32}$	1.954×10^{-24}	7.866×10^{-9}
	55.0	52.9	$(4.19\pm0.48)\times10^{-32}$	2.026×10^{-24}	2.069×10^{-8}
	60.0	57.8	$(1.53\pm0.11)\times10^{-31}$	2.083×10^{-24}	7.331×10^{-8}
^{nat}Yb	40.0	36.9	$(1.55\pm0.22)\times10^{-32}$	1.722×10^{-24}	9.001×10^{-9}
	42.5	39.3	$(4.52\pm0.56)\times10^{-32}$	1.796×10^{-24}	2.517×10^{-8}
	45.3	42.0	$(8.30\pm0.91)\times10^{-32}$	1.860×10^{-24}	4.462×10^{-8}
	50.0	46.6	$(1.20\pm0.07)\times10^{-30}$	1.965×10^{-24}	6.107×10^{-7}
	55.0	51.5	$(2.53\pm0.08)\times10^{-30}$	2.047×10^{-24}	1.236×10^{-6}
	60.0	56.4	$(8.90\pm0.31)\times10^{-30}$	2.112×10^{-24}	4.214×10^{-6}
	65.0	61.3	$(1.45\pm0.03)\times10^{-29}$	2.164×10^{-24}	6.701×10^{-6}

gy, E_f is the fission barrier, B_n is the neutron binding energy, A is the mass number of the compound nucleus and K_0 is a constant taken as 10.7 MeV ($K_0=\hbar^2/gmr_0^2$, where $g=2$ corresponding to the spin states of the neutron, m is the mass of the neutron, and r_0 is the radius parameter taken as 1.4×10^{-13} cm). The measured fission cross sections are mostly due to first chance fission in this region of the periodic table at moderate excitation energies (see the steep excitation functions; Fig. 1). Charged-particle emission can be ignored at these moderate excitation energies and hence the ratio of fission width to neutron emission width can be reasonably approximated to the ratio of fission cross section to total reaction cross section ($\Gamma_f/\Gamma_n \approx \sigma_f/\sigma_R$). The total reaction cross sections were calculated according to the optical model parameters of Huizenga and Igo [10] using the ALICE computer code [11]. A least-squares fitting procedure was used to fit the experimental Γ_f/Γ_n values to obtain "best values" of E_f, a_f, and a_n. The a_f values were floated from $A/8$ to $A/20$, which are reasonable upper and lower limits (see Fig. 2). The ratio of a_f/a_n was floated from 1.00 to 1.35 in increments of 0.01. E_f values were allowed to vary between 20 and 35 MeV, in increments of 0.1 MeV, which are reasonable lower and upper limits. By this procedure, the E_f values were calculated and "best values" of E_f, a_f, and a_f/a_n were selected on the basis of the minimum sum of the squares of the deviation (ψ^2). We have used the simplest form of the statistical-model expression [1] neglecting the angular momentum brought in by alpha particles, barrier penetration, pairing and shell corrections to the neutron binding energies, etc., because their contributions are expected to be very small. The results of these analyses are given in Tables II and III. It is obvious from Tables II and III that:

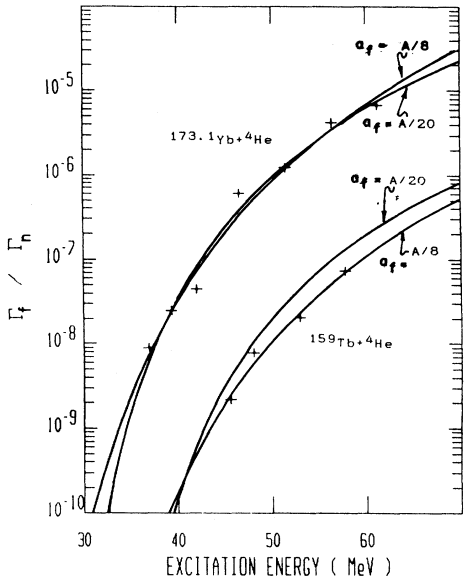

FIG. 2. Theoretical fits to the Γ_f/Γ_n data for the helium-ion-induced fission of terbium and ytterbium using a_f values $A/8$ and $A/20$.

(a) For $^{177.1}$Hf, E_f lies in the vicinity of 24.4–29.8 MeV, with corresponding a_f and a_n values in the ranges 22.1–8.9 MeV^{-1} and 19.9–8.1 MeV^{-1}, respectively. The a_f/a_n values vary between 1.11 and 1.10.

(b) For ^{163}Ho, E_f lies in the vicinity of 28.9–34.9 MeV, with corresponding a_f and a_n values in the ranges 20.4–8.2 MeV^{-1} and 19.8–8.2 MeV^{-1}, respectively.

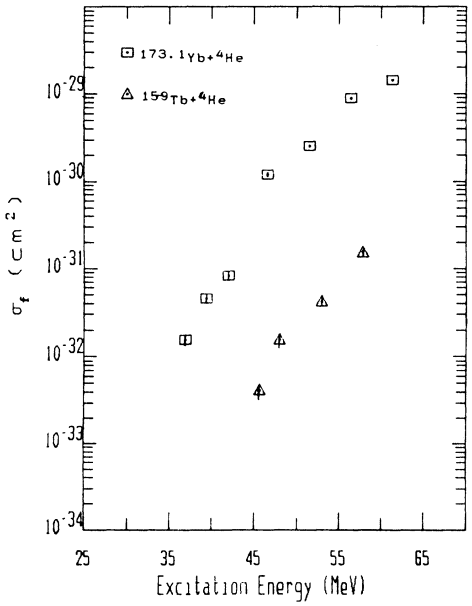

FIG. 1. Measured fission excitation functions for the helium-ion-induced fission of ytterbium and terbium.

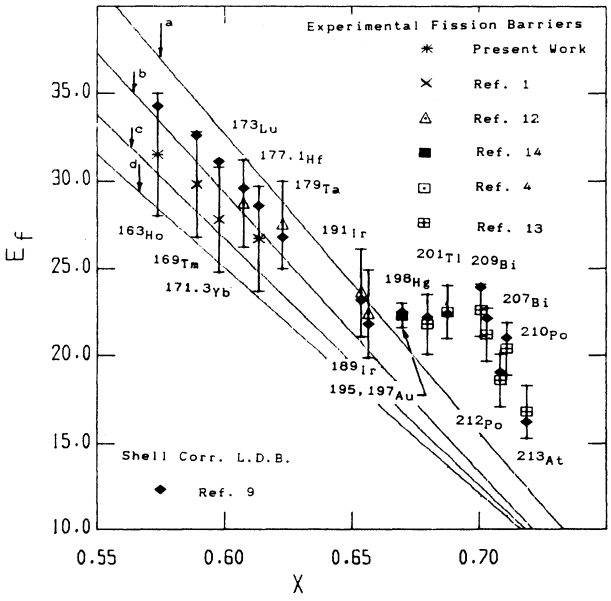

FIG. 3. Comparison of the measured and predicted fission barriers for low-Z systems (a=LDM [15], b=RLDM [16], c=RFRM [18], d=RFRM [17]).

TABLE II. Least-squares fit of the theoretical Γ_f/Γ_n expression to the experimental data on ^{159}Tb+^{4}He→^{163}Ho.

E_f (MeV)	a_f (MeV^{-1})	a_n (MeV^{-1})	a_f/a_n	ψ^2	Remarks
28.9	20.4	19.8	1.03	0.0246	$a_f=A/8$
29.5	18.1	17.8	1.02	0.0241	$A/9$
30.3	16.3	16.0	1.02	0.0238	$A/10$
30.8	14.8	14.7	1.01	0.0237	$A/11$
31.5	13.6	13.5	1.01	0.0233	$A/12$
31.9	12.5	12.5	1.00	0.0234	$A/13$
32.5	11.6	11.6	1.00	0.0239	$A/14$
33.7	10.2	10.2	1.00	0.0246	$A/16$
34.7	9.00	9.00	1.00	0.0286	$A/18$
34.9	8.2	8.2	1.00	0.2805	$A/20$

The a_f/a_n values vary between 1.03 and 1.00.

From these observations, the values of fission barrier for $^{177.1}$Hf and ^{163}Ho can be assigned to be 26.7±3.0 and 31.5±3.5 MeV, respectively. The uncertainties shown would allow for inclusion of other values derived from reasonable upper and lower limits of a_f and a_n values.

The experimental fission barriers of ^{163}Ho and $^{177.1}$Hf and a few other low-Z nuclides in the deformed and closed-shell region [1,4,12–14] were compared with fission barriers calculated by liquid-drop-based models such as the simple liquid-drop model (LDM) [15], shell-corrected liquid-drop model [9], rotating liquid-drop model (RLDM) [16], and finite-range models (RFRM) of Sierk [17] and Mustafa *et al.* [18]. The fission barriers based on the Sierk model [17] and RLDM of Cohen *et al.* [16] were calculated by the ALICE computer code [11] for nonrotating fissioning nuclei. The barriers based on the model of Mustafa *et al.* were read from the graph of Z^2/A versus fission barrier of beta stable nonrotating fissioning nuclei, given in their paper [18]. These theoretical and experimental fission barriers are summarized in Table IV and also illustrated in Fig. 3 where the fissionability parameter X is given by equation [19]:

$$X=\frac{Z^2/A}{50.883\{1-1.7826[(N-Z)/A]^2\}}\ , \tag{1}$$

TABLE III. Least-squares fit of the theoretical Γ_f/Γ_n expression to the experimental data on $^{173.1}$Yb+^{4}He→$^{177.1}$Hf.

E_f (MeV)	a_f (MeV^{-1})	a_n (MeV^{-1})	a_f/a_n	ψ^2	Remarks
24.4	22.1	19.9	1.11	0.1377	$a_f=A/8$
25.0	19.7	17.7	1.11	0.1342	$A/9$
25.6	17.7	16.0	1.11	0.1339	$A/10$
26.2	16.1	14.5	1.11	0.1337	$A/11$
26.7	14.8	13.3	1.11	0.1333	$A/12$
27.2	13.6	12.3	1.11	0.1337	$A/13$
27.7	12.6	11.4	1.11	0.1368	$A/14$
28.5	11.1	10.0	1.11	0.1366	$A/16$
29.1	9.8	8.9	1.10	0.1398	$A/18$
29.8	8.9	8.1	1.10	0.1438	$A/20$

where Z, N, and A are the proton, neutron, and mass numbers, respectively. It is seen that there is good agreement between the experimental fission barriers and those predicted by a semiempirical mass formulation based on the charged liquid drop for ^{163}Ho, $^{177.1}$Hf and other nuclei in the deformed region, such as ^{169}Tm, $^{171.3}$Yb [1], ^{173}Lu, ^{179}Ta, ^{191}Ir, and ^{189}Ir [12]. This indicates that ground-state deformation has very little, if any, effect on lowering of the fission barriers. It also suggests that the basic features of the simple liquid-drop theory are sufficiently accurate in describing the nuclides in this deformed region.

The ratios of level-density parameters at the saddle point to these at the ground state, a_f/a_n, obtained from an analysis of fission excitation functions of ^{163}Ho, $^{177.1}$Hf, and other nuclides in the deformed region [1,12] in terms of statistical-model expressions [5], were compared with other published data [4,13,14] on a_f/a_n ratios in the closed-shell region. This includes 16 nuclei ranging from ^{163}Ho to ^{213}At. The a_f/a_n ratio for ^{163}Ho, one of the lightest compound nuclei, was found to be 1.01. The maximum a_f/a_n ratio was found to be 1.50 at the Bi-At closed shell region [13]. A systematic trend was observed in the a_f/a_n ratio of these 16 nuclei (from ^{163}Ho to ^{213}At) as a function of Z^2/A (see Fig. 4) which can be represented by the equation

$$a_f/a_n=10.856-0.7046Z^2/A+0.012\,64(Z^2/A)^2\ . \tag{2}$$

It is obvious from Fig. 4 that the a_f/a_n ratio tends to decrease with Z^2A and approaches unity in the region of deformed nuclei (e.g., ^{163}Ho, ^{169}Tm, $^{171.3}$Yb, and ^{173}Lu). This may be expected since, as one moves away from closed-shell nuclei (e.g., the Au-Bi region) the ground state and saddle point have similar level structures [20] and therefore a_f and a_n tend to become equal [1].

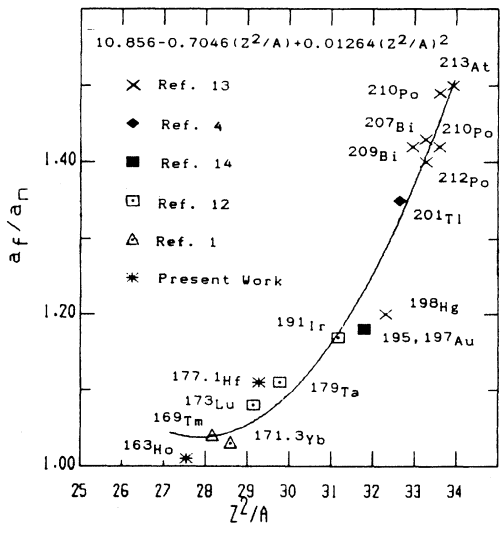

FIG. 4. Ratio of level-density parameters a_f/a_n as a function of Z^2/A.

TABLE IV. Experimental and theoretical fission barriers for some low-Z systems.

Compound nucleus (C.N.)	Expt. E_f (MeV)	LDM [15] (MeV)	RLDM [16] (MeV)	Shell-corr. LD [9] (MeV)	Sierk [17] (MeV)	Mustafa *et al.* [18] (MeV)	Ref.
^{163}Ho	31.5±3.5	36.98	33.6	34.3	28.4	30.5	This work
^{169}Tm	29.8±3.0	34.6	31.2	32.6	26.6	28.3	[1]
$^{171.3}$Yb	27.8±3.0	33.1	29.7	31.1	25.3	27.2	[1]
^{173}Lu	28.7±2.5	31.5	28.2	29.6	24.2	25.2	[12]
$^{177.1}$Hf	26.7±3.0	30.6	27.3	28.6	23.3	25.3	This work
^{179}Ta	27.5±2.5	28.9	25.7	26.8	22.1	23.3	[12]
^{189}Ir	22.4±2.5	22.9	20.0	21.8	17.6	17.8	[12]
^{191}Ir	23.6±2.5	23.5	20.5	23.2	18.0	19.0	[12]
^{195,197}Au	22.3±0.7	20.1	17.6	21.6	15.5	15.9	[14]
		20.7	18.1	23.4	15.9	17.5	
^{201}Tl	22.5±1.5	17.4	15.1	22.4	13.6	14.1	[4]
^{209}Bi	22.6±1.5	15.4	12.9	23.9	11.9	13.1	[13]
^{210}Po	20.4±1.5	13.8	11.8	21.0	10.8	11.1	[13]
^{213}At	16.8±1.5	12.7	10.9	16.2	9.9	10.0	[13]

Since the present experiment extends the range of nuclides for which fission excitation functions were obtained at moderate excitation energies, it will be interesting to study the dependence of $\Gamma_f\Gamma_n$ with Z^2/A at a constant excitation energy. In our earlier work [1], the $\log_{10}\Gamma_f/\Gamma_n$ values of ^{169}Tm and $^{171.3}$Yb at constant 40 MeV excitation energy appear to deviate slightly from the linear dependency on Z^2/A which is given by the equation [12]

$$\log_{10}\Gamma_f/\Gamma_n = 1.41Z^2/A - 49.8 \ . \quad (3)$$

It is observed that this may be due to uncertainties involved in the measurements of such low fission cross sections [1]. To understand this better, an analysis of the available data on $\log_{10}\Gamma_f/\Gamma_n$ at constant 40 MeV excitation energy from our work as well as those from the literature [1,4,12–14,21–23] for compound nuclei from ^{163}Ho to ^{213}At and ^{232}Th to ^{254}Fm was done. It was observed that the $\log_{10}\Gamma_f/\Gamma_n$ data in the ^{163}Ho to ^{213}At region where symmetric fission is predominant can be represented by the equation

$$\log_{10}\Gamma_f/\Gamma_n = 1.26Z^2/A - 44.77 \ . \quad (4)$$

All the nuclei in this region lie fairly close to the expected line (Fig. 5). However, in the actinide region ^{232}Th–^{254}Fm (all of which are predominantly asymmetric fission nuclei), only a relatively weak dependence of $\log_{10}\Gamma_f/\Gamma_n$ on Z^2/A was observed (see Fig. 5). The estimation of Γ_f/Γ_n in the heavy-element region is complicated by two factors; first, at this excitation energy the first chance fission represents only a small portion of the total fission probability. Secondly, because of the relatively large contribution of fission to the total reaction cross section, it is not possible to approximate Γ_n by σ_R. However, Γ_f/Γ_n is quite energy insensitive for these elements and, by indirect analysis [22,23], it has been possible to extract reasonable estimates of this ratio (in the Th to Fm region). The $\log_{10}\Gamma_f/\Gamma_n$ data in the actinide region can be represented by the equation

$$\log_{10}\Gamma_f/\Gamma_n = 0.366Z^2/A - 13.455 \ . \quad (5)$$

A theoretically more meaningful analysis may be the correlation of Γ_f/Γ_n with $E_f'-B_n'$ where E_f' and B_n' are the effective fission barrier and neutron binding energy, respectively. The values for Γ_f/Γ_n at 40 MeV, and the effective fission barrier E_f', were taken directly from the experimental determinations [1,4,9,12–14,21,22] because any necessary corrections to E_f are inherent in the measured thresholds. The effective values for the neutron

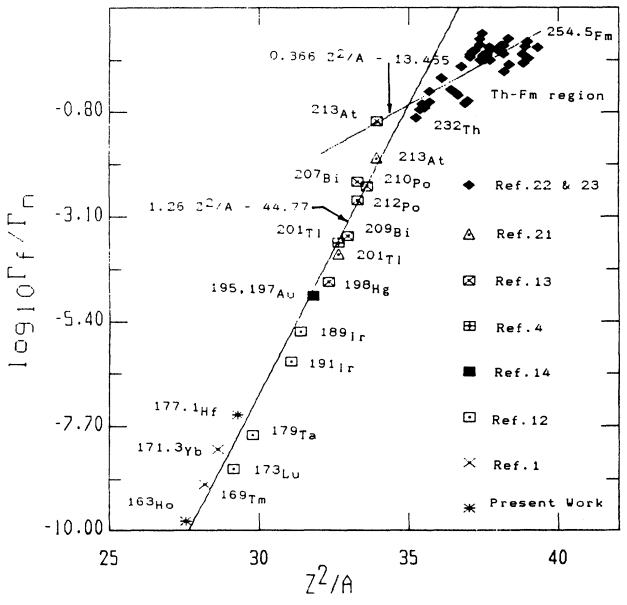

FIG. 5. Correlation of the logarithm of fission to neutron-emission width ratios with Z^2/A at an excitation energy of 40 MeV for different compound nuclei. The logarithms are to the base 10. (The Th–Fm region includes 44 nuclei; only the first and last nuclei are labeled for the sake of clarity).

binding energy B_n' were obtained by assuming

$$\text{even-even}\quad B_n'=B_n+\Delta p^n+\Delta S^n\ ,$$

$$\text{even-odd}\quad B_n'=B_n+\Delta S^n\ ,$$

$$\text{odd-odd}\quad B_n'=B_n-\Delta p^n+\Delta S^n\ ,$$

where B_n is the ordinary neutron binding energy, Δp^n is the pairing energy correction ($\pm 11/A^{1/2}$), ΔS^n is the shell correction (taken as a positive value for ground states lying below the reference mass surface) and the even-odd characteristics refer to the residual nucleus after neutron emission. The values of B_n and ΔS^n were taken from Ref. [9]. The $\log_{10}\Gamma_f/\Gamma_n$ values were plotted with $E_f'-B_n'$, in which B_n' includes (a) no shell correction but only a pairing energy term (sum of squares of deviation $=7.84$), (b) full shell correction including pairing energy term (sum of squares of deviation $=2.68$), and (c) 50% shell correction with pairing energy term (sum of squares of deviation $=1.79$; Fig. 6). Based on the minimum sum of squares of deviation, the 50% shell correction with pairing energy term was found to be the best and the data can be represented by the following equation:

$$\log_{10}\Gamma_f/\Gamma_n=1.593-0.452(E_f'-B_n')\ . \tag{6}$$

The results suggest that shell effects tend to persist even at higher excitation energies, and in the deformed region the linear dependency of $\log_{10}\Gamma_f/\Gamma_n$ with $E_f'-B_n'$ is not significantly affected by shell corrections to the effective neutron binding energy because of its small magnitude.

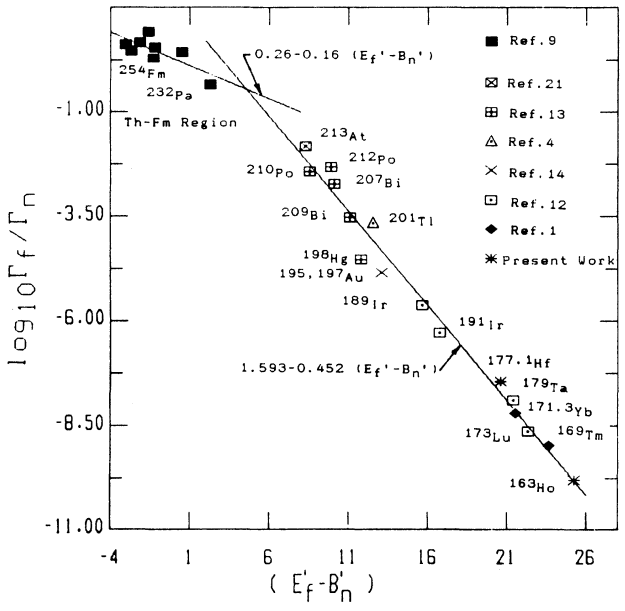

FIG. 6. Correlation of the logarithm of fission to neutron-emission width ratios with $E_f'-B_n'$ (B_n' includes 50% shell correction with pairing energy term) at an excitation energy of 40 MeV for different compound nuclei. The logarithms are to the base 10. (The Th–Fm region includes 8 nuclei; only the first and last nuclei are labeled for the sake of clarity).

The 50% shell correction would be a reasonable estimate at excitation energies involved in this comparison, and those values have been adopted in this analysis.

From Figs. 5 and 6, it appears that the linear dependency of $\log_{10}\Gamma_f/\Gamma_n$ with Z^2/A and $E_f'-B_n'$ starts deviating in the Ra region where symmetric and asymmetric fission barriers are comparable. Above Ra (from Th to Fm) the symmetric fission barrier is greater than the asymmetric fission barrier, hence these are essentially asymmetric fission nuclei. Below Ra, the asymmetric fission barrier is greater than symmetric fission barrier (predominantly symmetric fission). The recent careful study of Itkis *et al.* [24] indicates that asymmetry of mass distribution is present below the Ra region and disappears somewhat abruptly near $A=200$. Based on this fact, it can be assumed that Eqs. (4) and (6) essentially represent symmetric fission. On combining Eqs. (4) and (6) the following equation is obtained.

$$E_f'-B_n'=102.57-2.79Z^2/A\ . \tag{7}$$

If one neglects, or averages out shell effects, and assumes B_n' to be approximately constant, then

$$E_f=K_1-K_2(Z^2/A)\ , \tag{8}$$

where K_1 and K_2 are constants. This is the same form given by Cohen and Swiatecki [15] for obtaining the barrier of a charged liquid drop. Since Eq. (7) represents symmetric fission, the E_f' in the above equation can be assumed to be $E_{f\,(\text{symmetric})}'$. The symmetric fission barriers obtained from the above equation were compared with the experimental symmetric fission barriers available in literature from a phenomenological analysis of the probability of symmetric and asymmetric fission of nuclei (kinetic energy measurements) [24–26] and from an analysis of fission excitation functions [1,4,9,12–14] and are given in Table V. It is obvious from these results that the symmetric fission barriers obtained from Eq. (7) are reasonably close to experimentally observed fission barriers. However, this type of analysis is not capable of obtaining asymmetric fission barriers by extrapolating fission barriers of actinide nuclides (predominantly asymmetric fissioning nuclei). The main reason behind this may be that although the asymmetric fission barrier in the actinide region is lower than the symmetric fission barrier, it may be comparable in magnitude. Hence the average fission barrier obtained by analysis of excitation functions may not essentially represent the asymmetric fission barriers. The available experimental data on asymmetric fission barriers [24–26] was plotted against Z^2/A. From the limited available data on asymmetric fission barriers, it is apparent that asymmetric fission barrier ($E_{f\,(\text{asy})}'-B_n'$) is linearly dependent on Z^2/A. Based on the available data, the asymmetric fission barrier can be represented by the equation.

$$E_{f\,(\text{asym})}'-B_n'=235.11-6.65Z^2/A \tag{9}$$

From Table V, it appears that near $A=200$ the asymmetric fission barrier becomes higher than the symmetric

TABLE V. Symmetric and asymmetric fission barriers.

Nuclide	Symm. fission barrier [from Eq. (7)] (MeV)	Expt. symm. fission barrier (MeV)	Asymm. fission barrier [from Eq. (9)] (MeV)	Expt. asymm. fission barrier (MeV)	Average expt. fission barrier[a] (MeV)	Ref.
^{163}Ho	31.66		57.90		31.5	This work
^{169}Tm	30.01		53.90		29.8	[1]
$^{171.3}$Yb	29.00		51.14		27.8	[1]
^{173}Lu	27.62		47.68		28.7	[12]
$^{177.1}$Hf	27.01		46.57		26.7	This work
^{201}Tl	21.47		28.02		22.5	[4]
^{210}Po	20.67	21.2	23.51	24.4	20.4	[13,24]
^{213}At	15.43	17.3	17.04	19.8	16.8	[13,24]
^{227}Ra	11.89	9.3	12.06	7.95		[25]
^{226}Ac	8.65	8.8	5.98	7.80		[25]
^{227}Ac	9.59	8.5	7.45	7.40		[25]
		8.5		7.30		[26]
^{228}Ac	9.02	8.8	7.47	7.0		[25]
		9.2		7.2		[26]
^{232}Th	9.93		7.71		5.95	[9]
^{233}Th	9.50		7.87		6.44	[9]
^{232}Pa	6.87		1.65		6.18	[9]
^{238}U	8.26		3.54		5.80	[9]

[a]Obtained by the analysis of fission excitation functions.

fission barrier. Thus asymmetric fission may not be experimentally observable below $A=200$ and hence it disappears around $A=200$ [24]. The average fission barriers of actinide nuclei, obtained by analysis of excitation functions, lie between asymmetric and symmetric fission barriers (see Table V) and indicate that the average fission barriers of actinide nuclei do not represent the asymmetric fission barriers uniquely.

The rather impressive correlation obtained in Eqs. (7) and (9) is gratifying and tends to lend credence to the assumptions that have been used.

We appreciate the help and cooperation extended to us by Dr. S. N. Chintalapudi, V. S. Pandit, and the operating staff of the Variable Energy Cyclotron (VEC) Calcutta, in carrying out the cyclotron irradiations.

[1] R. H. Iyer, A. K. Pandey, P. C. Kalsi, and R. C. Sharma, Phys. Rev. C **44**, 2644 (1991).
[2] R. D. Evans, *The Atomic Nucleus* (McGraw-Hill, New York, 1955), p. 172.
[3] D. L. Hill and J. A. Wheeler, Phys. Rev. **89**, 1102 (1953).
[4] D. S. Brunett, R. C. Gatti, F. Plazil, P. B. Price, W. J. Swiatecki, and S. G. Thompson, Phys. Rev. **134**, B952 (1964).
[5] R. Vandenbosch and J. R. Huizenga, *Nuclear Fission* (Academic, New York, 1973).
[6] K. G. Kuvatov, V. N. Okolovich, L. A. Smirina, G. N. Smirenkin, V. P. Bochin, and V. S. Romanov, Yad. Fiz. **14**, 79 (1971) [Sov. J. Nucl. Phys. **14**, 45 (1972)].
[7] T. Sikkeland, Phys. Rev. **135**, B669 (1964).
[8] A. K. Pandey, R. C. Sharma, P. C. Kalsi, and R. H. Iyer, *Proceedings of the DAE Symposium on Nuclear Physics* (B.A.R.C., Bombay, 1991), Vol. 34B, p. 213.
[9] W. D. Myers and W. J. Swiatecki, Lawrence Radiation Laboratory Report No. UCRL/11980, 1965.
[10] J. R. Huizenga and G. J. Igo, Nucl. Phys. **29**, 462 (1962).
[11] M. Blann, LLNL Report No. UCID 19614, 1982.
[12] G. M. Raisbeck and J. W. Cobble, Phys. Rev. **153**, 1270 (1967).
[13] A. Khodai-Joopari, University of California Radiation Laboratory, Report No. UCRL-16489, 1966.
[14] R. L. Brodzinski and J. W. Cobble, Phys. Rev. **172**, 1194 (1968).
[15] S. Cohen and W. J. Swiatecki, Ann. Phys. (N.Y.) **22**, 406 (1963).
[16] S. Cohen, F. Plasil, and W. J. Swiatecki, Ann. Phys. **82**, 557 (1974).
[17] A. J. Sierk, Phys. Rev. C **33**, 2039 (1986).
[18] M. G. Mustafa, P. A. Baisden, and H. Chandra, Phys. Rev. C **25**, 2524 (1982).
[19] B. B. Back, R. R. Betts, J. E. Gindler, B. D. Wilkins, S. Saini, M. B. Tsang, C. K. Gelbke, W. G. Lynch, M. A. McMahan, and P. A. Baisden, Phys. Rev. C **32**, 195 (1985).
[20] A. Bohr, *Proceedings of the First United Nations International Conference on Peaceful Uses of Atomic Energy*, Geneva, 1955 (United Nations, New York, 1956), Paper P/911, Vol. 2.
[21] J. R. Huizenga, R. Chaudhry, and R. Vandenbosch, Phys. Rev. **126**, 210 (1962).
[22] R. Vandenbosch and J. R. Huizenga, in *Proceedings of the Second United Nations International Conference on the*

Peaceful Uses of Atomic Energy, Geneva, 1958 (United Nations, Geneva, 1958), Paper P/688, Vol. 15, p. 284.

[23] J. E. Gindler, G. L. Bate, and J. R. Huizenga, Phys. Rev. **136**, B1333 (1964).

[24] M. G. Itkis, V. N. Okolovich, A. Ya. Rusanov, and G. H. Smirenkin, Fiz. Elm. Chastits At. Yadra **19**, 701 (1988) [Sov. J. Part. Nucl. **19**, 301 (1988)].

[25] G. A. Kudyaev, Yu. B. Ostapenko, and G. N. Smirenkin, Yad. Fiz. **45**, 1534 (1987) [Sov. J. Nucl. Phys. **45**, 951 (1987)].

[26] E. Konecny, H. J. Specht, J. Weber, in *Proceedings of 3rd IAEA Symposium on the Physic and Chemistry of Fission,* Rochester, New York, 1973 (IAEA-SM-174/20, Vienna, 1974), Vol. 2, p. 3.